THE EFFECT OF THREE-BODY INTERACTIONS ON THE LIQUID-LIQUID PHASE COEXISTENCE OF BINARY FLUID MIXTURES

Richard J. Sadus

Computer Simulation and Physical Applications Group, School of Computer Science and Software Engineering, Swinburne University of Technology, PO Box 218, Hawthorn, Victoria 3122, Australia

Keywords: theory, molecular simulation, three-body interactions, liquid-liquid equilibria, binary mixtures

Abstract

The Gibbs ensemble algorithm is implemented to determine the liquid-liquid phase coexistence of binary fluid mixtures interacting via a two-body Lennard-Jones + three-body Axilrod-Teller potential. The contributions of both two-body and three-body interactions are calculated exactly. This is the first time that three-body interactions have been incorporated rigorously in a molecular simulation of a binary mixture. The addition of the Axilrod-Teller term can affect liquid-liquid miscibility substantially. In particular, Axilrod-Teller interactions have a large effect on the densities of the coexisting liquid phases.

1. Introduction

Theories of liquids have almost invariably assumed that intermolecular interactions are limited to pairs of molecules. Calculations of fluid properties [1] ignore routinely the contributions of three- or more-body interactions. However, the available evidence [2-7] suggests that the effect of three-body interactions may be important in some circumstances. For example, it is reported [8] typically that a two-body plus an Axilrod-Teller potential [9] improves the prediction of third virial coefficients of atomic systems. Three-body interactions also appear to have a greater role in molecular fluids [3,4]. Nevertheless, the exact role of three-body interactions remains unclear partly because attempts to account for three-body interactions commonly involve approximations. Furthermore, previous work on three-body interactions has been confined almost exclusively to pure fluids.

In principle, molecular simulation can be used to calculate three-body interactions rigorously. However, the use of molecular simulation has been restricted largely to pairwise interactions, and the few studies [2,3,10-13] that have attempted to include three-body interactions have relied on various approximations rather than rigorous calculation. For example, simulations have been reported [12,13] which estimate the contribution of three-body effects via periodic calculation of three-body interactions. Recently [14], Gibbs ensemble simulation has been used to calculate exactly the effect of three-body interactions on the vapour-liquid equilibria of pure fluids. The results [14] indicate that Axilrod-Teller interactions can alter significantly

the density of the liquid branch of the coexistence curve. This suggests that three-body interactions may have a significant effect on liquid-liquid equilibria.

The aim of this work is to investigate the effect of three-body interactions on the liquid-liquid equilibria of binary mixtures. The Gibbs ensemble [15] is used to calculate the liquid-liquid phase coexistence of binary mixtures with components interacting via a Lennard-Jones + Axilrod-Teller intermolecular potential. The calculation of three-body interactions is exact with both two- and three-body interactions contributing to the acceptance criterion of each and every attempted Monte Carlo move. This is the first time that three-body interactions have been incorporated rigorously in a molecular simulation of a binary mixture.

2. Theory

2.1 Intermolecular Potential

The intermolecular potential (u) is the sum of contributions from two-body interactions($u(ij)$) and three-body dispersion interactions ($u(ijk)$).

$$u = u(ij) + u^{disp}(ijk) \tag{1}$$

The Lennard-Jones potential was used to calculate interactions between pairs of molecules separated by a distance r_{ij}

$$u(ij) = 4\varepsilon\left[\left(\frac{\sigma}{r_{ij}}\right)^{12} - \left(\frac{\sigma}{r_{ij}}\right)^{6}\right] \tag{2}$$

where the ε and σ parameters are characteristic of the strength of intermolecular interaction and molecular size, respectively.

The Axilrod-Teller term [9] accounts for the contribution of three-body dispersion interactions

$$u^{disp}(ijk) = \frac{\nu\left(1 + 3\cos\theta_i \cos\theta_j \cos\theta_k\right)}{\left(r_{ij} r_{ik} r_{jk}\right)^3} \tag{3}$$

where θ refers to the inside angles of a triangle (see Fig. 1) formed by three molecules i, j and k, and ν is the nonadditive coefficient. This potential is negative for near-linear configurations and positive for acute triangular arrangements.

2.2 Potential Parameters

The calculations were performed in reduced units relative to component 1. The parameters for the Lennard-Jones potentials were $\varepsilon_{22}/\varepsilon_{11} = 0.75$, $\sigma_{22}/\sigma_{11} = 0.95$, $\varepsilon_{12} = 0.7\sqrt{\varepsilon_{11}\varepsilon_{22}}$ and $\sigma_{12} = (\sigma_{11} + \sigma_{22})/2$. This combination of parameters was chosen because earlier work [16] indicated that they are associated with liquid-liquid equilibria in a binary mixture of Lennard-Jones molecules.

For the Axilrod-Teller potential, we must consider the nonadditive coefficient arising from triplets composed of different combinations of the component molecules. There are four distinct possible combinations of three molecules in a binary mixture. The nonadditive coefficient of component 2 molecules was related to component 1 by

$$\nu_{222} = \alpha \nu_{111} \tag{4}$$

where α is an arbitrary adjustable parameter. A value of $\frac{\nu_{111}}{\varepsilon_{11}\sigma_{11}^{9}} = 0.0712$ was used which corresponds to the nonadditive coefficient of an atom such as argon [17]. The unlike nonadditive coefficients were obtained by taking a geometric average of the like interactions.

$$\nu_{112} = \sqrt[3]{\nu_{111}\nu_{111}\nu_{222}} \tag{5}$$

$$\nu_{122} = \sqrt[3]{\nu_{111}\nu_{222}\nu_{222}} \tag{6}$$

2.3 Simulation Details

The NPT-Gibbs ensemble [15] was used to simulate the coexistence of two liquid phases. A total of 200 molecules were partitioned between two boxes to simulate the two coexisting liquid phases. The temperature of the entire system was held constant and surface effects were avoided by placing each box at the centre of a periodic array of identical boxes. Equilibrium was achieved by attempting molecular displacements (for internal equilibrium), volume fluctuations (for mechanical equilibrium) and particle interchanges between the boxes (for material equilibrium).

The simulations were performed in cycles with each cycle consisting of 200 attempted displacements, a single volume fluctuation, and 500 interchange attempts. The maximum molecular displacement and volume changes were adjusted to obtain, where possible, a 50% acceptance rate for the attempted move. Ensemble averages were accumulated only after the system had reached equilibrium. The equilibration period was typically 2500 cycles and a further 2500 cycles was used to accumulate the averages. The calculations were truncated at intermolecular separations greater than half the box length, and appropriate long-range corrections [18] were used to obtain the full contribution of pair interactions to energy and pressure. The full (untruncated) three-body potential was calculated to avoid uncertainties that arise when calculating three-body long-range corrections from unknown pair-distribution functions. Alternative computational approaches for long-range corrections are available [19].

The contributions of both two-body and three-body interactions to the configurational energy of the fluid were recalculated for each attempted move and the configurational properties were updated after each successful move. Therefore, changes to both two-body and three-body interactions contributed to the acceptance criterion and the predicted phase coexistence curve is the result of two-body and three-body interactions. A typical run required approximately 57 CPU hours on a Cray YMP-EL and 9 CPU hours on a Fujitsu VPP300 supercomputer.

2.4 Estimating Critical Properties

Gibbs ensemble simulations cannot be used to determine directly the critical point. However, the critical temperature T_c* and critical composition can be estimated by fitting the simulation data to the following relationships

$$x_\beta - x_\alpha = C\left|1 - \frac{T^*}{T_c^*}\right|^{0.32} \tag{7}$$

and

$$\frac{x_\beta + x_\alpha}{2} = A(T^* - T_c^*) + B \tag{8}$$

The critical density can be obtained by using the density analogues of Eqs (7) and (8).

3. Results

The liquid-liquid coexistence data obtained from molecular simulation are summarised in Tables 1 and 2. The normal convention was adopted for the reduced density ($\rho^* = \rho\sigma^3$), temperature ($T^* = kT/\varepsilon$), energy ($E^* = E/\varepsilon$), pressure ($P^* = P\sigma^3$) and chemical potential ($\mu^* = \mu/\varepsilon$). The chemical potential was determined from the equation proposed by Smit and Frenkel [20]. The data in Table 1 are for $\alpha = 1$ and results for $\alpha = 0.5$ are included in Table 2. In Tables 1 and 2 the contribution of Lennard-Jones (LJ) and Axilrod-Teller (AT) interactions to both the energy and pressure are identified. A value of P* = 1 was used in both cases to ensure a reasonably high density for the coexisting liquid phases. The estimated critical properties are summarized in Table 3.

4. Discussion

Exact calculations of three-body interactions in fluids are rare because of the very large increase in computation required compared with two-body calculations. Typically, two-body Gibbs ensemble simulations are reported with between three to five hundred molecules. However, to feasibly conduct three-body calculations, we have limited the simulations to two hundred molecules.

When $\alpha = 1$, the nonadditive three-body coefficients for the two components are identical and all the mixed three-body interactions are also identical. The calculated

coexistence properties for a binary mixture of this type are summarised in Table 1 and the temperature-composition behaviour is illustrated in Fig. 2. The data in Table 1 indicate that Axilrod-Teller interactions typically represent between 5% and 6% of the Lennard-Jones contribution to the energy of either liquid phase. The overall contribution of the Axilrod-Teller term is positive thereby increasing the energy of the liquid phases. Furthermore, the contribution of the Axilrod-Teller term to pressure outweighs the contribution from the Lennard-Jones potential. The comparison of the composition-temperature behaviour of this mixture with the Lennard-Jones fluid in Fig. 2 indicates that the effect of three body interactions is to shift the coexistence curve to substantially lower temperatures. In particular, the calculated critical temperature (Fig. 2 and Table 3) is substantially lower than the critical temperature of the Lennard-Jones fluid. If we assume that the critical temperature is a qualitative indicator of the degree of miscibility (i.e., the critical temperature increases with decreasing miscibility), the effect of three-body interactions in this case is to increase the miscibility of the mixture. However, it should be noted that in this case, the magnitude of the nonadditive coefficient assigned to component 2 is unrealistically high in view of the fact that component 2 has substantially weaker two body interactions than component 1.

The nonadditive dispersion coefficient (v) of a molecule is proportional to the additive dispersion coefficient ($C_6 = 4\varepsilon\sigma^6$). In view of the fact that $\varepsilon_{22}/\varepsilon_{11} = 0.75$, a value of $\alpha = 0.5$ gives a more realistic description of the relative nonadditive coefficient for the two components. The calculations for $\alpha = 0.5$ are summarised in Table 2. The data in Table 2 show that the Axilrod-Teller term typically contributes 4% of the Lennard-Jones contribution to the energy of the coexisting liquid phases. The contribution of the Axilrod-Teller term to both energy and pressure is positive and its contribution to pressure outweighs the contribution from the Lennard-Jones potential. The temperature-coexistence behaviour illustrated in Fig. 2 indicates that the Axilrod-Teller term reduces substantially the composition range for two-phase coexistence but two-phase coexistence is observed at considerably higher temperatures. This latter point is exemplified by a substantial increase in the critical temperature compared with the Lennard-Jones mixture (Fig. 2 and Table 3).

The temperature-density behaviour of the Lennard Jones + Axilrod Teller and Lennard-Jones [16] mixtures is illustrated in Fig. 3. It is apparent from Fig. 3 that the addition of the Axilrod-Teller term reduces substantially the densities of the coexisting phases. The shift to lower densities partly offsets the increase in repulsion from three-body interactions. This is consistent with earlier work [17] for a one-component fluid which demonstrated that Axilrod-Teller interactions reduce substantially the density of the liquid branch of the vapour-liquid coexistence curve. When $P^* = 1$, the densities of the two coexisting phases of the Lennard-Jones mixture are similar at all temperatures. In contrast, the addition of the Axilrod-Teller term increases the density difference between the coexisting phases. Therefore, liquid-liquid immiscibility in the Lennard-Jones + Axilrod-Teller mixtures is observed for a larger range of densities than is observed in the Lennard-Jones mixture.

What are the implications of these results for real fluids? The answer to this question depends primarily on the adequacy of Axilrod-Teller term to model three-body interactions. The Axilrod-Teller potential only represents the contribution of dipoles to three body interactions. Other higher multipole terms can also contribute to three body interactions but their effect is generally negligible [4,6]. Further, there is evidence [21] that the effect of higher multipole terms is offset by a fourth order triple-dipole term. Consequently, the triple-dipole term as represented by the Axilrod-Teller potential, is likely to be a good representation of three-body dispersion interactions. However, the Axilrod-Teller potential only accounts for attractive dispersion interactions. In reality, repulsive interactions from three-body overlap are also possible. Rittger [4] suggested that repulsive overlap could potentially explain inaccuracies in the analysis of some thermodynamic data for xenon. Sadus and Prausnitz [9] reported that the contribution to the configurational energy of three-body attraction is offset substantially by contributions from three-body repulsion, as represented by the electrostatic distortion model [22].

5. Conclusions

For the first time, three-body interactions have been incorporated rigorously in a molecular simulation of a binary mixture. Three-body dispersion interactions can

potentially have a significant effect on the liquid-liquid equilibria of binary mixture. The exact nature of the effect depends on the relative magnitude of three-body interactions with respect to two-body dispersion interactions. In the absence of any compensating three-body repulsion or other interactions, the most probable effect of the Axilrod-Teller term is to decrease substantially the liquid-liquid miscibility of binary mixtures. In particular, the densities of the coexisting liquid phases are affected significantly by the Axilrod-Teller term.

List of symbols

A	fitting parameter in Eq. (8); phase identifier
B	fitting parameter in Eq. (8); phase identifier
C	fitting parameter in Eq. (7)
c	critical property
E	configurational energy
k	Boltzmann's constant
P	pressure
r	intermolecular distance
T	temperature
u	intermolecular potential
v	nonadditive coefficient
x_1	mole fraction of component 1

Greek Alphabet

α	adjustable parameter
ε	Lennard-Jones energy parameter
σ	Lennard-Jones distance parameter
ρ	number density
θ	intramolecular angle

Subscripts and Superscripts

*	reduced property
AT	Axilrod-Teller
disp	dispersion

i, j, k molecule i, j or k

LJ Lennard-Jones

l liquid

v vapour

Acknowledgement

The simulations were performed on the Swinburne University of Technology's Cray YMP-EL computer and the Australian National University Supercomputer Centre's Fujitsu VPP300 supercomputer.

References

[1] R.J. Sadus, High Pressure Phase Behaviour of Multicomponent Fluid Mixtures, Elsevier, Amsterdam, 1992.

[2] J.A. Barker, R.A. Fischer and R.O. Watts, Mol. Phys., 21 (1971) 657-673.

[3] A.P. Monson, M. Rigby and W.A. Steele, Mol. Phys., 49 (1983) 893-898.

[4] M.J. Elrod and R.J. Saykally, Chem. Rev., 94 (1994) 1975-1997.

[5] E. Rittger, Mol. Phys., 69 (1990) 853-865.

[6] E. Rittger, Mol. Phys., 69 (1990) 867-894.

[7] E. Rittger, Mol. Phys., 71 (1990) 79-96.

[8] J.A. Barker, C.H.J. Johnson, and T.H. Spurling, Aust. J. Chem., 25 (1972) 1813-1814.

[9] B.M. Axilrod and E. Teller, J. Chem. Phys., 11 (1943) 299-300.

[10] Y. Miyano, Fluid Phase Equilib., 95 (1994) 31-43.

[11] B. Smit, T. Hauschild, and J.M. Prausnitz, Mol. Phys., 77 (1992) 1021-1031.

[12] R.J. Sadus and J.M. Prausnitz, J. Chem. Phys., 104 (1996) 4784-4787.

[13] R.J. Sadus, Fluid Phase Equilib., 116 (1996) 289-295.

[14] R.J. Sadus, Fluid Phase Equilib. (1997), in press.

[15] A.Z. Panagiotopoulos, N. Quirke, M. Stapleton and D.J. Tildesley, Mol. Phys., 63 (1988) 527-545.

[16] R.J. Sadus, Mol. Phys., 89 (1996) 1187-1194.

[17] P.J. Leonard, and J.A. Barker, in H. Eyring and D. Henderson (Eds), Theoretical Chemistry: Advances and Perspectives, Vol. 1, Academic Press, New York, 1975.

[18] M.P. Allen, M.P. and D.J. Tildesley, Computer Simulation of Liquids, Clarendon, Oxford, 1987.

[19] E. Rittger, Comp. Phys. Commun., 67 (1992) 412-434.

[20] B. Smit and D. Frenkel, D., Mol. Phys., 68 (1989) 951.

[21] J.A. Barker, C.H.J. Johnson, and T.H. Spurling, Aust. J. Chem., 25 (1972) 1811-1812.

[22] A.E. Sherwood, A.G. de Rocco and E.A. Mason, J. Chem. Phys., 44 (1966) 2984-2994.

Table 1

Gibbs-ensemble simulation of liquid-liquid equilibria at P* = 1 using the Lennard-Jones + Axilrod-Teller intermolecular potential with $\alpha = 1$.†

Liquid Phase A

T^*	ρ^*	x_1	$-E^*_{LJ}$	E^*_{AT}	$-P^*_{LJ}$	P^*_{AT}	μ^*_1	μ^*_2
0.955	0.763(8)	0.884(36)	4.84(15)	0.25(1)	0.38(9)	0.57(2)	2.64	1.53
0.96	0.764(13)	0.902(42)	4.93(25)	0.25(2)	0.33(11)	0.58(4)	2.59	1.47
0.97	0.750(15)	0.807(27)	4.41(15)	0.23(1)	0.25(15)	0.53(4)	2.48	1.44
0.99	0.751(15)	0.814(72)	4.50(35)	0.24(2)	0.31(9)	0.53(5)	2.41	1.39
1.0	0.731(15)	0.589(167)	3.70(45)	0.20(1)	0.20(6)	0.44(4)	2.54	1.32

Liquid Phase B

T^*	ρ^*	x_1	$-E^*_{LJ}$	E^*_{AT}	$-P^*_{LJ}$	P^*_{AT}	μ^*_1	μ^*_2
0.955	0.721(22)	0.170(28)	3.07(11)	0.21(1)	0.29(7)	0.45(4)	2.79	1.46
0.96	0.717(22)	0.158(40)	3.04(10)	0.21(2)	0.28(5)	0.45(5)	2.82	1.49
0.97	0.720(19)	0.186(59)	3.07(10)	0.21(1)	0.30(8)	0.45(4)	2.71	1.39
0.99	0.724(16)	0.244(67)	3.08(6)	0.20(2)	0.21(9)	0.43(4)	2.56	1.35
1.0	0.720(14)	0.418(174)	3.33(30)	0.19(1)	0.22(3)	0.42(3)	2.52	1.31

†Values in parentheses indicate the uncertainty in the last digit.

Table 2

Gibbs-ensemble simulation of liquid-liquid equilibria at P* = 1 using the Lennard-Jones + Axilrod-Teller intermolecular potential with $\alpha = 0.5$.†

Liquid Phase A								
T^*	ρ^*	x_1	$-E^*_{LJ}$	E^*_{AT}	$-P^*_{LJ}$	P^*_{AT}	$-\mu^*_1$	$-\mu^*_2$
0.97	0.758(10)	0.847(85)	4.64(36)	0.23(2)	0.25(10)	0.52(6)	2.59	1.57
0.99	0.747(18)	0.778(119)	4.34(49)	0.20(3)	0.24(9)	0.46(8)	2.47	1.47
1.02	0.732(10)	0.781(90)	4.21(34)	0.19(2)	0.19(7)	0.42(5)	2.50	1.57
1.04	0.732(13)	0.725(64)	4.01(23)	0.17(1)	0.16(9)	0.39(4)	2.47	1.45
1.08	0.707(5)	0.683(60)	3.75(17)	0.16(1)	0.16(5)	0.33(2)	2.61	1.52

Liquid Phase B								
T^*	ρ^*	x_1	$-E^*_{LJ}$	E^*_{AT}	$-P^*_{LJ}$	P^*_{AT}	$-\mu^*_1$	$-\mu^*_2$
0.97	0.742(14)	0.358(31)	3.32(10)	0.131(10)	0.09(8)	0.29(2)	2.58	1.53
0.99	0.736(16)	0.349(51)	3.24(8)	0.124(5)	0.08(12)	0.27(2)	2.57	1.45
1.02	0.713(15)	0.358(48)	3.10(8)	0.115(5)	0.07(7)	0.25(2)	2.57	1.57
1.04	0.712(10)	0.310(67)	3.06(8)	0.114(5)	0.11(6)	0.24(1)	2.59	1.46
1.08	0.691(7)	0.317(60)	3.97(6)	0.110(4)	0.06(7)	0.23(1)	2.49	1.51

†Values in parentheses indicate the uncertainty in the last digit.

Table 3

Estimated liquid-liquid critical properties†

v^*_{111}	α	P^*_c	T^*_c	ρ^*_c	$x_c(1)$
0.0712	1	1	1.01	0.732	0.500
0.0712	0.5	1	1.148	0.650	0.430
0	0	1	1.112	0.728	0.494

† Data for the Lennard-Jones mixture (v^*_{111} = 0, α = 0) are from the literature [16].

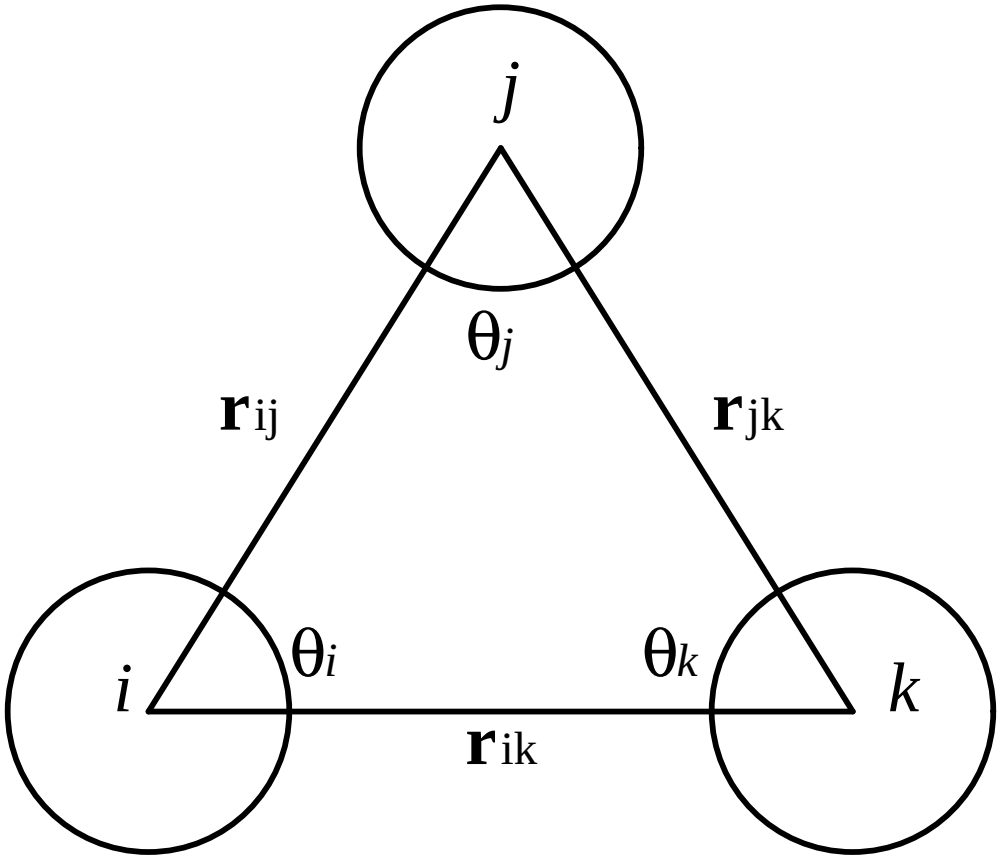

Fig. 1. Triplet configuration of atoms i, j and k in Eq. (3).

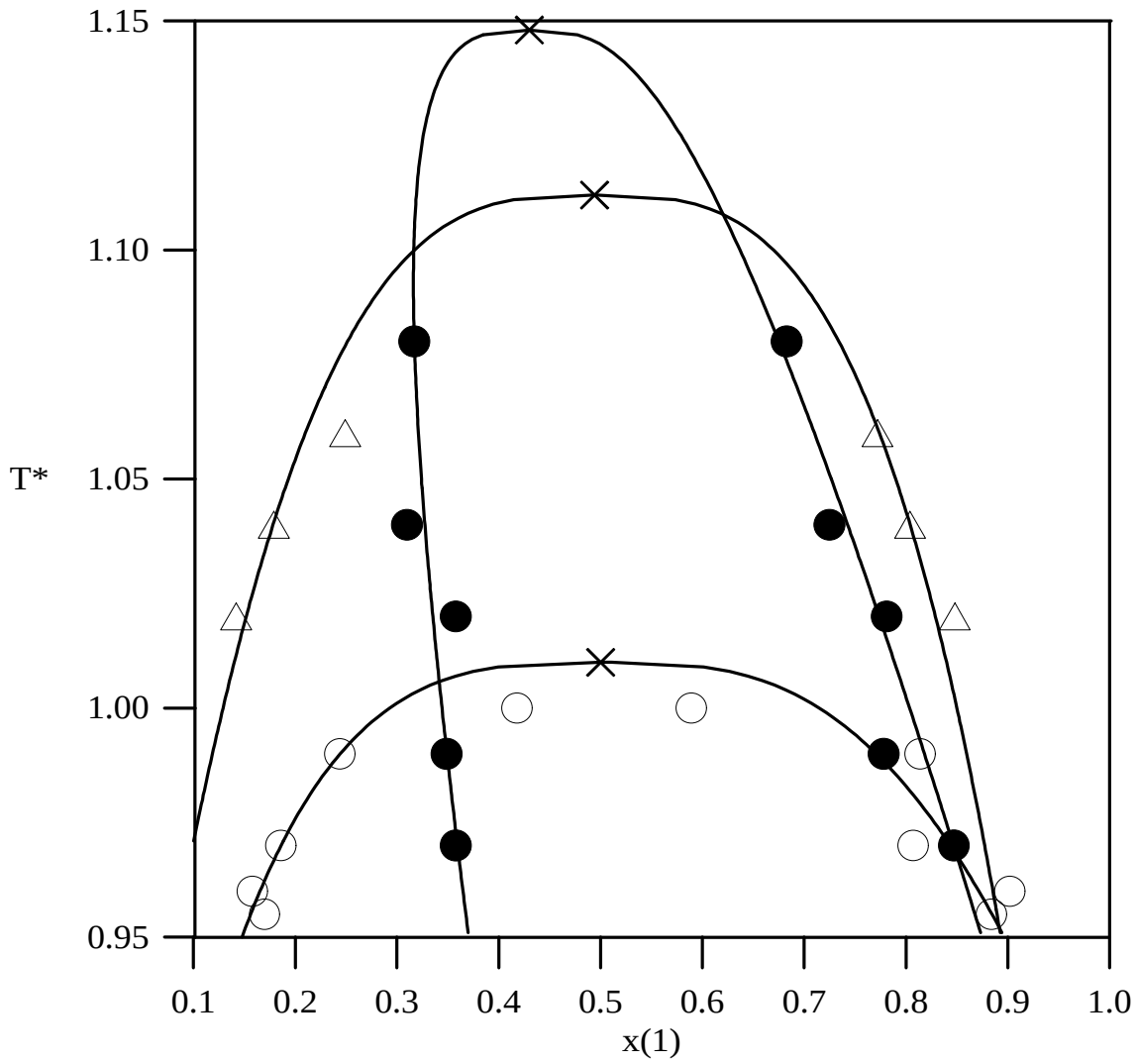

Fig. 2. The temperature-composition projection at P* = 1 for binary mixtures exhibiting liquid-liquid equilibria. Results are shown for calculations using the Lennard-Jones potential (Δ, [16]) and the Lennard-Jones + Axilrod-Teller potential with $\alpha = 1$ (○) and $\alpha = 0.5$ (●). The solid lines were obtained from fitting the simulation data to the critical exponent relationships (Eqs (7) and (8)). The estimated critical point is identified (×).

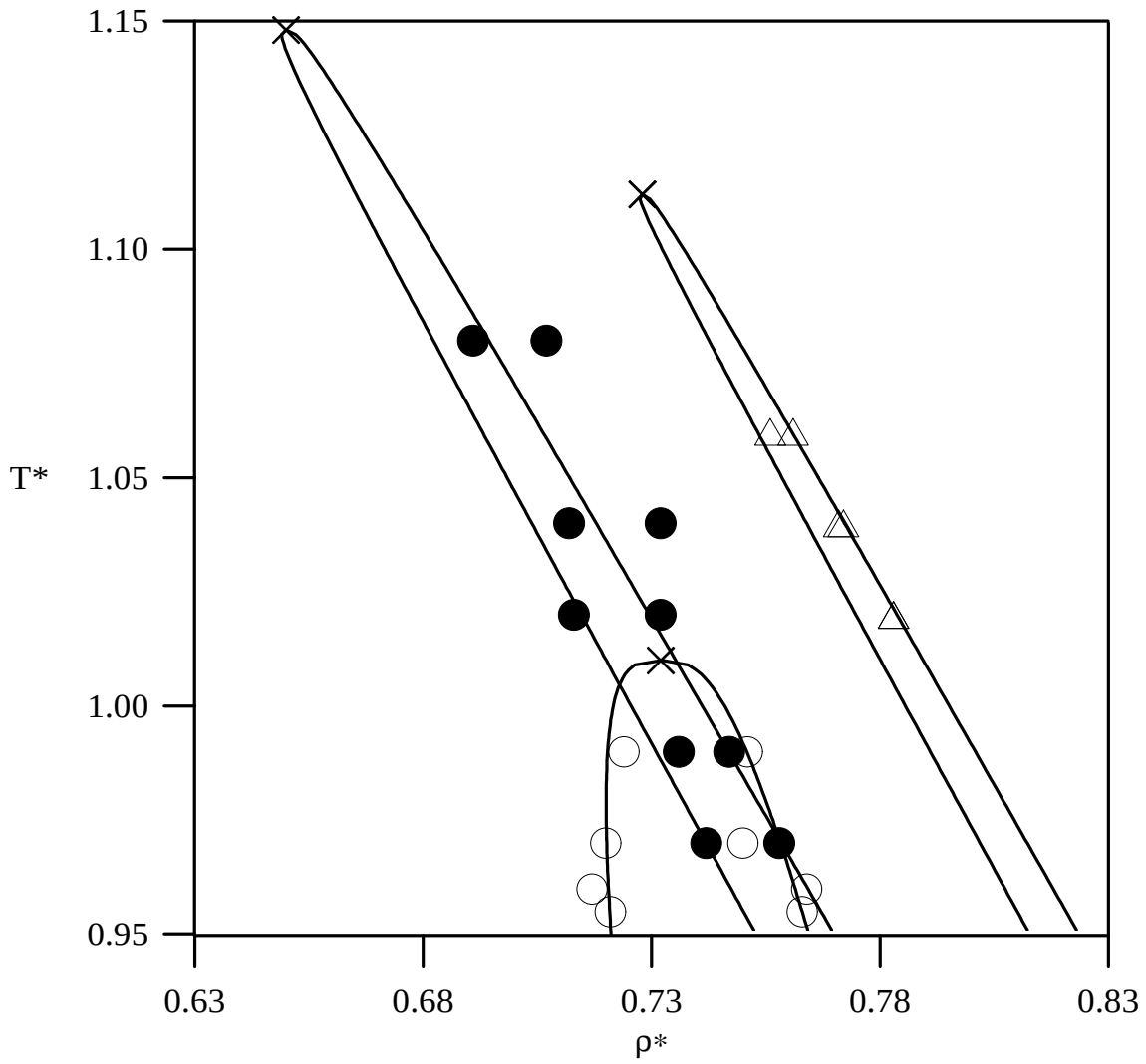

Fig. 3. The temperature-density projection at P* = 1 for binary mixtures exhibiting liquid-liquid equilibria. Results are shown for calculations using the Lennard-Jones potential (Δ, [16]) and the Lennard-Jones + Axilrod-Teller potential with α = 1 (○) and α = 0.5 (●). The solid lines were obtained from fitting the simulation data to the critical exponent relationships (Eqs (7) and (8)). The estimated critical point is identified (×).